Journal of Zhejiang University-SCIENCE B (Biomedicine & Biotechnology) *2024 25(7):617-627*
www.jzus.zju.edu.cn; www.springer.com/journal/11585
E-mail: jzus_b@zju.edu.cn

Research Article

https://doi.org/10.1631/jzus.B2300929

Check for updates

Prediction of peritoneal free cancer cells in gastric cancer patients by golden-angle radial sampling dynamic contrast-enhanced magnetic resonance imaging

Xueqing YIN[1]✉, Xinzhong RUAN[1], Yongmeng ZHU[1], Yongfang YIN[1], Rui HUANG[1], Chao LIANG[2]

[1]*The First Affiliated Hospital of Ningbo University, Ningbo 315000, China*
[2]*Ningbo Medical Center Lihuili Hospital, Ningbo 315000, China*

Abstract: Objective: Peritoneal free cancer cells can negatively impact disease progression and patient outcomes in gastric cancer. This study aimed to investigate the feasibility of using golden-angle radial sampling dynamic contrast-enhanced magnetic resonance imaging (GRASP DCE-MRI) to predict the presence of peritoneal free cancer cells in gastric cancer patients. Methods: All enrolled patients were consecutively divided into analysis and validation groups. Preoperative magnetic resonance imaging (MRI) scans and perfusion were performed in patients with gastric cancer undergoing surgery, and peritoneal lavage specimens were collected for examination. Based on the peritoneal lavage cytology (PLC) results, patients were divided into negative and positive lavage fluid groups. The data collected included clinical and MR information. A nomogram prediction model was constructed to predict the positive rate of peritoneal lavage fluid, and the validity of the model was verified based on data from the verification group. Results: There was no statistical difference between the proportion of PLC-positive cases predicted by GRASP DCE-MR and the actual PLC test. MR tumor stage, tumor thickness, and perfusion parameter Tofts-Ketty model volume transfer constant (K_{trans}) were independent predictors of positive peritoneal lavage fluid. The nomogram model featured a concordance index (*C*-index) of 0.785 and 0.742 for the modeling and validation groups, respectively. Conclusions: GRASP DCE-MR could effectively predict peritoneal free cancer cells in gastric cancer patients. The nomogram model constructed using these predictors may help clinicians to better predict the risk of peritoneal free cancer cells being present in gastric cancer patients.

Key words: Gastric cancer; Magnetic resonance; Golden-angle radial sampling; Nomogram model; Peritoneal free cancer cells

1 Introduction

Gastric cancer cases in China are still ranked among the top five of all cancers regarding incidence and mortality (Wu et al., 2019). Peritoneal metastasis is among the main factors affecting the prognosis of patients with gastric cancer (Mezhir et al., 2010; Riihimäki et al., 2016). Positive peritoneal lavage cytology (PLC) has been proven to be the strongest independent predictor of patient survival (Japanese Gastric Cancer Association, 2011). Currently, PLC is the most accurate diagnostic method for detecting free cancer cells in the peritoneal cavity (Jamel et al., 2018). A strategy of prioritizing chemotherapy can be adopted to convert PLC status to negative before performing radical surgery, which can greatly benefit patient survival (Japanese Gastric Cancer Association, 2021; Valletti et al., 2021). However, the application of preoperative chemotherapy is still limited due to the invasive nature of peritoneal lavage, which is usually performed during surgical procedures. Although the staging of the tumor before surgery has been attempted by conventional computed tomography (CT) and magnetic resonance imaging (MRI) based on tumor size and surrounding conditions, small intraperitoneal metastases are still easily overlooked, resulting in undesirable outcomes (Huang et al., 2015; Borggreve et al., 2019; Xu et al., 2019). Therefore, it is necessary to evaluate the presence of peritoneal micrometastases by noninvasive methods before operation.

✉ Xueqing YIN, yinxueqing301@163.com
Xueqing YIN, https://orcid.org/0009-0000-1377-736X

Received Dec. 21, 2023; Revision accepted Mar. 21, 2024;
Crosschecked May 17, 2024; Published online June 5, 2024

© Zhejiang University Press 2024

Previous basic and clinical studies have demonstrated that tumor hemodynamics are associated with tumor aggressiveness and distant metastasis (Oh-E et al., 2001; Offersen et al., 2003). The mechanism of peritoneal metastasis in gastric cancer is still unclear (Sun et al., 2017). The "seed and soil" theory has been recognized as the basic theory of gastric cancer metastasis (Yashiro et al., 1996), which states that free cancer cells in the peritoneal cavity form metastatic foci in this environment, forming the basis of peritoneal metastasis in gastric cancer. Traditional imaging examinations are limited to morphologic assessment that cannot determine the presence of peritoneal micrometastases or free cancer cells. Previous studies have suggested that free cancer cells in gastric cancer can spread to the peritoneum through hematogenous metastasis or directly detach from the tumor and implant in the peritoneum (To et al., 2003). Tumor angiogenesis largely affects tumor growth and metastatic pathways (Weidner, 1998; Wang et al., 2007). The dynamic contrast-enhanced (DCE)-MRI technique can reflect the permeability and perfusion status of tumor microvessels through perfusion parameters (Teo et al., 2014; Feng, 2022). The Pharmacokinetics and Pharmacodynamics Technical Committee and Imaging Committee of the American Center for Experimental Cancer Medicine reviewed and discussed the situation of DCE-MRI in early clinical trials and recommended the use of DCE-MRI to evaluate the vascular situation of tumors (Leach et al., 2012). A new, enhanced scanning technology from Siemens, the golden-angle radial sampling (GRASP) technique of MRI can obtain high temporal resolution images and quantitative data for drug metabolism kinetic modeling, providing valuable data for tumor invasion assessment (Chandarana et al., 2013; Feng et al., 2014).

This study intended to investigate the feasibility of predicting PLC-positive probability using GRASP DCE-MRI, in an attempt to provide a new non-invasive auxiliary precision diagnosis method for gastric cancer.

2 Materials and methods

2.1 Research subjects

We prospectively collected data of gastric cancer patients who were hospitalized and treated at a gastrointestinal surgery facility (The First Affiliated Hospital of Ningbo University, Ningbo, China) from January 2020 to June 2022. The inclusion criteria were: (1) diagnosis of gastric cancer confirmed by gastroscopy and biopsy pathology; (2) absence of distant metastases confirmed by contrast-enhanced abdominal CT or other imaging examinations; and (3) no history of antitumor therapies. The exclusion criteria were: (1) unsuitable for MRI examination; (2) patients with failed MRI data acquisition or poor image quality that could not be analyzed; and (3) distant metastases detected by MRI examination.

During the study period, the data of a total of 127 gastric cancer patients with surgical indications were collected, of which three patients with MRI contraindications, one patient with incomplete pathological data, and two patients with distant metastases found by MRI were excluded, resulting in a cohort of 121 (95.3%) patients. The first 70% of patients included in the study (according to the time of their visit) were designated as the modeling group, which included 55 males and 30 females with a median age of 63 years (53–81 years). The remaining 30% were designated as the validation group, which was set up to verify the reliability of the model. This group included 19 males and 17 females with a median age of 65 years (59–80 years). The difference in age, gender, hypertension, or diabetes incidence was not significant between patients in the modeling group and the validation group (P>0.05).

Patients in the modeling group were divided into a negative lavage fluid subgroup (negative subgroup) and a positive lavage fluid subgroup (positive subgroup) according to the result of cytological test. The difference in age, gender, hypertension, or diabetes incidence was not significant (P>0.05) between patients in the negative subgroup and the positive subgroup (Table 1).

Basic patient data included age, gender, and whether or not hypertension or diabetes were present. Laboratory test data contained postoperative pathological grade and tumor type. All the above data were collected in the electronic medical records system.

2.2 GRASP DCE-MRI

All enrolled patients underwent GRASP DCE-MRI before surgery, and the obtained MRI images were analyzed. According to the MRI data, the preoperative tumor-node-metastasis (TNM) imaging staging of gastric cancer was performed. Preoperative

Table 1 Comparison of characteristics and parameters between positive and negative subgroups

Characteristic	Total	Positive subgroup	Negative subgroup	Test value	*P* value
Case load (*n* (%))	85	16 (18.8)	69 (81.2)		
Age (years)	63 (53–81)	64 (54–77)	62 (48–79)	0.566[a]	0.574
Gender (male (%))	55 (64.7)	10 (11.8)	45 (52.9)	2.773[b]	0.096
Hypertension (*n* (%))	32 (37.6)	18 (21.2)	14 (16.5)	0.83[b]	0.975
Diabetes (*n* (%))	24 (28.2)	11 (12.9)	13 (15.3)	1.24[b]	0.500
Thickness (mm)		3.03±2.75	2.61±1.98	7.43[c]	<0.05
Perfusion parameter					
K_{trans} (min^{-1})		0.32±0.18	0.28±0.27	−0.793[c]	0.006
K_{ep} (min^{-1})		1.82±1.28	1.83±1.70	−0.026[c]	0.144
V_e		0.19±0.09	0.16±0.10	−0.209[c]	0.107
iAUC		0.13±0.06	0.12±0.07	0.238[c]	0.037
T stage (*n* (%)), A/B*					
T_2	9 (10.6)/8 (9.4)	0/0	9 (10.6)/8 (9.4)	13.78[d]/	<0.001/
T_3	27 (31.8)/29 (34.1)	5 (5.9)/4 (4.7)	22 (25.9)/25 (29.4)	11.16[d]	<0.001
T_4	49 (57.6)/48 (56.5)	11 (12.9)/11 (12.9)	38 (44.7)/37 (43.5)		
N stage (*n* (%)), A/B*					
N_0	29 (34.1)/28 (32.9)	6 (7.0)/6 (7.0)	23 (27.1)/22 (25.9)	1.158[d]/	0.245/
N_1	35 (41.2)/40 (47.0)	7 (8.2)/9 (10.6)	28 (32.9)/31 (36.5)	0.306[d]	0.857
N_2	21 (24.7)/17 (20.0)	3 (3.5)/3 (3.5)	18 (21.2)/14 (16.4)		
Histological grade (*n* (%))					
Low differentiated	18 (21.2)	5 (5.9)	13 (15.3)	−0.117[d]	0.206
Medium-low	24 (28.2)	4 (4.7)	20 (23.5)		
Medium	12 (14.1)	2 (2.4)	10 (11.8)		
Medium-high	22 (25.9)	3 (3.5)	19 (22.4)		
Highly	9 (10.6)	2 (2.4)	7 (8.2)		
Lauren classification (*n* (%))					
Intestinal type	17 (20.0)	2 (2.4)	15 (17.6)	9.051[b]	<0.05
Diffuse type	37 (43.5)	10 (11.8)	27 (31.8)		
Mixed type	16 (18.8)	4 (4.7)	12 (14.1)		

[a] *Z* value of *U* test; [b] χ^2 value of χ^2 test; [c] *t* value of *t*-test; [d] *H* value of Kruskal-Wallis (K-W) rank sum test; * A is TN stage of magnetic resonance imaging (MRI) diagnosis, and B is TN stage of postoperative pathology. K_{trans}: Tofts-Ketty model volume transfer constant; K_{ep}: rate constant; V_e: extravascular volume; iAUC: incremental area under curve.

peritoneal lavage fluid was collected and cytological tests were conducted.

The study used the Vida 3.0T MRI Magnetom (Siemens, Germany) and a 64-channel abdominal coil. Patients were asked to fast for 6 h before the examination, and 10–15 min prior to the examination, they were intramuscularly administered 10 mg of atropine sulfate injection (654-2, Hangzhou Minsheng Pharmaceutical Co., Ltd., China). Patients were then instructed to drink 500–1000 mL of warm water to fill their stomach before the scan. They were asked to take the supine position with the head first, and the coil center was placed approximately 3 cm below the xiphoid process. The scanning parameters included conventional spin-echo sequence axial T1-weighted imaging (T1WI), T2WI, diffusion-weighted imaging (DWI) sequence, coronal and sagittal T2WI, and axial and coronal enhanced T1WI. The scanning parameters were as follows: T1WI, repetition time (TR) 3.5–4.2 ms, echo time (TE) 1.23–2.57 ms; T2WI, TR 1400–6500 ms, TE 44–107 ms; DWI sequence, TR 6500–8400 ms, TE 44–120 ms. The slice thickness was 3 mm, the slice interval was 1 mm, the matrix was 256×256, and the scanning field was 380 mm×380 mm. The number of layers was determined based on the actual size of the gastric cavity. GRASP scanning was chosen for the enhanced scan, with scanning parameters of T1WI (TR 3.5 ms, TE 1.23 ms) and other axial T1WI sequences. The contrast agent was gadolinium-diethylenetriamine penta-acetic acid (Gd-DTPA), with

a dose of 0.1 mmol/kg, administered via a high-pressure injector through the elbow vein at a flow rate of 2 mL/s. Axial T1WI scans were performed immediately after contrast agent injection, and the total GRASP scanning time was about 5 min, resulting in 40 phases of reconstructed images.

The patient MRI images were analyzed and diagnosed on the eWord Picture Archiving and Communication System (PACS) V4 (Tomorrow Medical Network Technology Co., Ltd., Ningbo, China) by two diagnostic radiologists with more than ten years of experience each for the TNM staging of gastric cancer and excluding patients with $>M_0$. If the two radiologists had inconsistent judgments, a third diagnostician with more than 20 years of experience would be invited to jointly interpret the images.

A radiologist with more than five years of experience measured the maximum thickness of the tumor on the GRASP DCE sequence, which is the maximum thickness perpendicular to the tangent of the tumor and the adjacent normal gastric wall, on the PACS system. The average value of the two measurements or more than three times was taken if the mass had irregular borders, and the two or three measurements of the same lesion were taken at different time. The 40 phase images were imported into the MR Tissue 4D post-processing module for image post-processing using Verio Magnetom (Siemens, Germany), and the edge of the gastric cancer lesion was manually outlined as the region of interest (ROI) for the solid tumor, avoiding areas such as large blood vessels, cystic degeneration, and necrosis. Using the classic drug metabolism kinetics model (Bell et al., 2011), i.e., the Tolfs model, the software automatically calculated the perfusion parameters of the selected ROI at different rate modes: Tofts-Ketty model volume transfer constant (K_{trans}), extravascular volume (V_e), rate constant (K_{ep}), and incremental area under curve (iAUC), as shown in Fig. 1. The perfusion parameter values under slow mode were selected, three different planes of the lesion were outlined for each case, and the average value of each parameter was calculated.

2.3 Preoperative collection and peritoneal lavage fluid detection

The patient was placed in a head-low and foot-high position. After entering the abdominal cavity and locating the tumor position, but before the start of radical gastrectomy, the transverse mesocolon was lifted, 500 mL of physiological saline (37 °C) was injected into the upper region of the transverse colon around the stomach, and the lavage fluid was suctioned out of the stomach, spleen, and liver using a negative pressure aspirator and then aspirated into a clean specimen bag. If ascites were present, they were directly withdrawn and mixed with the peritoneal lavage fluid for examination.

The peritoneal fluid specimens were tested within 1 h after collection. The PLC test results and diagnostic criteria were as follows: the results were divided into two categories, positive and negative, according to

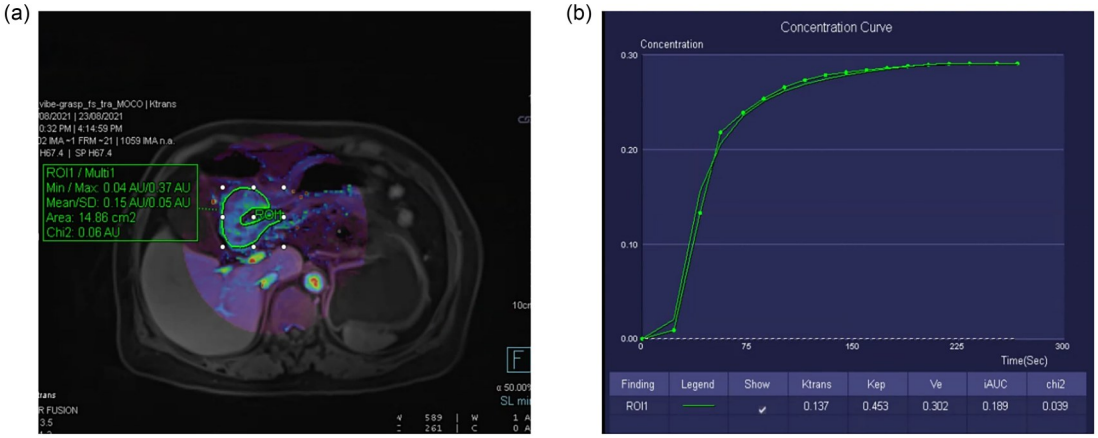

Fig. 1 Diagrams of ROI and concentration cure. (a) The manually delineated ROI of the tumor GRASP DCE sequence, with green (ROI1) representing the tumor region. (b) The time–concentration curve and perfusion parameter values of the local area of the tumor. ROI: regions of interest; GRASP: golden-angle radial sampling; DCE: dynamic contrast-enhanced; K_{trans}: Tofts-Ketty model volume transfer constant; K_{ep}: rate constant; V_e: extravascular volume; iAUC: incremental area under curve.

whether cancer cells were detected under a microscope. Positive results were recorded when cancer cells were found under the microscope, and negative results were obtained when cancer cells were absent, with only a few atypical cells visible, or other exclusionary positive results.

2.4 Study design

The differences between patients in the modeling group and the validation group were compared with regards to basic data, MR perfusion parameters, tumor thickness, TNM staging of MRI, and postoperative pathological results. Then, a nomogram prediction model was constructed to predict the positive rate of PLC, and the validity of the model was verified by data from the verification group. A flowchart of the whole study design is briefly shown in Fig. 2.

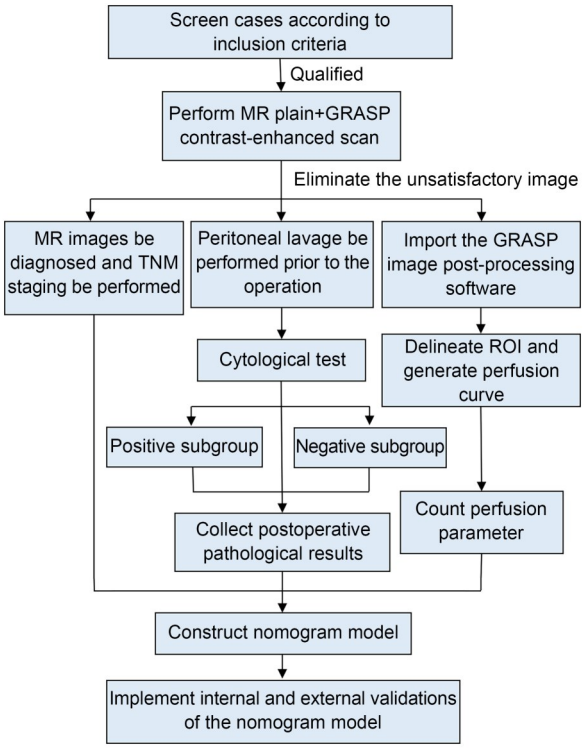

Fig. 2 Schematic diagram of study design. MR: magnetic resonance; GRASP: golden-angle radial sampling; TNM: tumor node metastasis; ROI: region of interest.

In order to obtain the accuracy of model data, we also compared the difference and correlation of variables between the positive subgroup and the negative subgroup in the experimental group, and gradually screened meaningful variables for analysis.

2.5 Statistical analysis

Statistical analysis was conducted using SPSS 25.0 software (IBM Corp, NY, USA). Count data were expressed as frequency (percentage), while normally distributed metric data were expressed as mean± standard deviation (SD). Comparisons between the PLC-positive and -negative groups were conducted using *t*-tests for normally distributed data, and median (quartile) was used for non-normally distributed data. The Kolmogorov-Smirnov (K-S) test was employed to determine if variables were normally distributed, while the homogeneity of variance was assessed by Levene's test. The Kruskal-Wallis (K-W) rank sum test was chosen for categorical data. Binary logistic regression analysis was performed to identify independent predictive factors affecting PLC positivity, where the multicollinearity diagnosed and weakly correlated variables were removed using stepwise regression. The obtained significant prediction factors were used to build a nomogram, which was drawn using the rms function of the software package R 4.1.0. Receiver operating characteristic (ROC) curve and concordance index (*C*-index) were implemented to measure the differentiation. The *C*-index calibration chart Hosmer-Lemeshow test and decision curve analysis (DCA) were utilized in the prediction group and the verification group, respectively, to verify the efficiency of the nomogram. Values of $P<0.05$ indicated statistically significant differences.

3 Results

3.1 Comparison of the results of PLC test and predictand by GRASP DCE-MRI

Among all enrolled patients, the number of positive PLC test results was 23 (19.0%) by a laboratory test, and the number of positive PCL test results predicted by GRSP DCE-MRI was 20 (16.5%), with no statistical difference between them ($\chi^2=7.26$, $P=0.95$). Specific data were presented in Table 2.

3.2 Comparison of PLC-positive rate between the modeling group and the validation group

No significant difference was established in the positive rate of PLC between the modeling group and the validation group (16/85 (18.8%) vs. 7/36 (19.4%),

Table 2 Comparison of positive number predicted by GRASP MRI and PLC test results

GRASP MRI-predicted value	Testing result		
	PLC-positive	PLC-negative	Summation
PLC-positive	19 (15.7%)	1 (0.8%)	20 (16.5%)
PLC-negative	4 (3.3%)	97 (80.2%)	101 (83.5%)
Summation	23 (19.0%)	98 (81.0%)	121 (100.0%)

GRASP: golden-angle radial sampling; MRI: magnetic resonance imaging; PLC: peritoneal lavage cytology.

χ^2=0.801, P=0.371). In the modeling group, the agreement rates of MRI T stage and postoperative pathological stage and MRI N stage and postoperative pathological stage were 97.6% (83/85) and 94.1% (80/85), respectively. The positive rate of peritoneal lavage fluid in the modeling group was 18.8% (16/85). There was no significant difference in age (P=0.574), gender (P=0.096), hypertension (P=0.975), diabetes (P=0.500), or N stage (P=0.245) between the positive and negative subgroups. There were significant differences in the perfusion parameters of K_{trans}, iAUC, tumor thickness, Lauren classification, MRI T stage, and pathological T stage between the positive and negative subgroups (P<0.05), which were determined as potential predictive factors for PLC positivity, as shown in Table 1.

3.3 Multivariate analysis of PLC positivity in the modeling group

Multivariate analysis was conducted on PLC positivity in the modeling group. Variables with P<0.05 in Table 1 were analyzed by univariate binary logistic regression to evaluate the correlation between each variable and PLC positivity. The results showed that K_{trans}, iAUC, tumor thickness, and MRI T stage were all correlated with PLC positivity. Variables with P<0.05 were selected by stepwise regression for bidirectional screening, and iAUC (r=0.96) with multicollinearity with K_{trans} was eliminated. The remaining variables were further included in multivariate binary logistic regression analysis. The results showed that K_{trans}, tumor thickness, and MRI T stage were still correlated with PLC positivity (P<0.05). The data for all the logistic regression results were presented in Table 3. The variance inflation factor values of these variables in the collinearity test were all less than 5, indicating that there was no multicollinearity among them, and that K_{trans}, tumor thickness, and MRI T stage were independent risk factors for PLC positivity.

3.4 Construction and validation of a prediction model for peritoneal carcinomatosis

A nomogram was constructed to predict peritoneal carcinomatosis in gastric cancer, using the three aforementioned factors (Fig. 3). A perpendicular line was drawn towards the point line from each predictor to identify the specific value of each variable. The total score was calculated by adding the matching points for each parameter in the nomogram, which was then transformed into a probability of PLC positivity. For example, in patients with MRI T stage of 4 and K_{trans} of 0.5 min^{-1}, the mass thickness was 30 mm and the total score was 90, corresponding to a positive predictive value of >90%.

The C-index of the nomogram model was 0.785 (95% confidence interval (CI): 0.574–0.869), and internal validation using bootstrap resampling with

Table 3 Univariate and multivariate logistic regression analyses of peritoneal lavage cytology (PLC)-positive predictors

Variate	Univariate logistic regression		Multivariate logistic regression	
	OR (95% CI)	P	OR (95% CI)	P
Age	0.972 (0.866–1.265)	0.784		
K_{trans} (min^{-1})	0.100 (0.009–0.168)	0.020	1.185 (0–2.029)	0.006
K_{ep} (min^{-1})	1.262 (0.594–3.032)	0.533		
V_e	0.920 (0.558–1.623)	0.036		
iAUC	1.772 (0.653–2.987)	0.048		
Thickness	1.040 (1.000–1.082)	0.032	1.933 (0.854–0.981)	0.029
Gender	0.807 (0.209–2.633)	0.453		
T stage	2.400 (2.130–4.693)	<0.001	0.003 (0–0.673)	0.023
N stage	1.225 (1.063–0.856)	0.010	0.549 (0.383–5.692)	0.543
Histological grade	0.574 (0.421–2.718)	0.428		
Lauren classify	1.732 (0.993–3.085)	0.047	0.816 (0.462–1.433)	0.525

OR: odds ratio; CI: confidence interval; K_{trans}: Tofts-Ketty model volume transfer constant; K_{ep}: rate constant; V_e: extravascular volume; iAUC: incremental area under curve.

1000 iterations yielded a calibration plot with an index of 0.746 (>0.7), indicating good predictive performance. The calibration plot and Hosmer-Lemeshow test (χ^2=2.59, P=0.738) for the validation group demonstrated high predictive accuracy of the nomogram (Fig. 4).

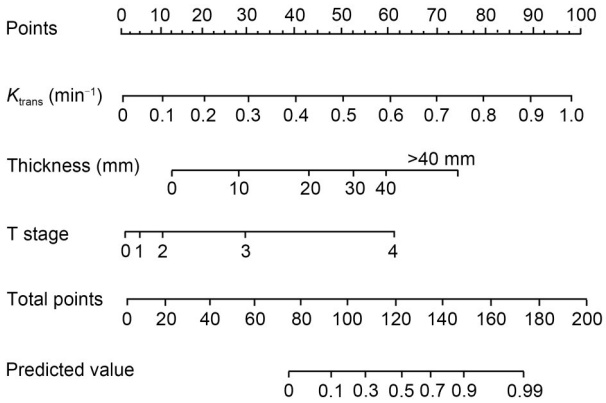

Fig. 3 Nomograms for prediction of peritoneal lavage cytology (PLC)-positive rate in patients with gastric cancer.

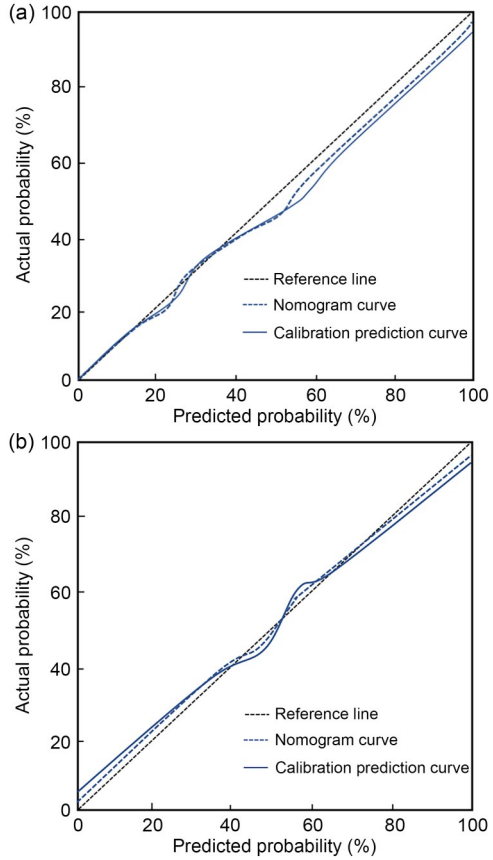

Fig. 4 Calibration charts of the nomogram model predicting positive peritoneal lavage cytology (PLC) of gastric cancer patients. (a) Modeling group; (b) Validation group.

External validation using the validation dataset showed a *C*-index of 0.742 (95% CI: 0.632–0.845) for the model, indicating good discrimination ability. ROC and DCA showed a good clinical utility of the nomogram model (Figs. 5 and 6).

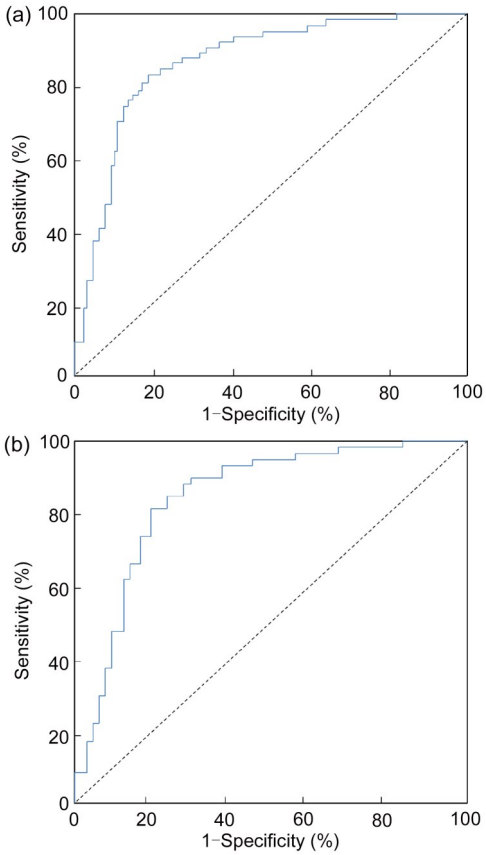

Fig. 5 Receiver operating characteristic curves of positive peritoneal lavage cytology (PLC) of gastric cancer patients predicted by nomogram model. (a) Modeling group; (b) Validation group.

4 Discussion

In this study, we explored the applicability of MRI images with higher soft tissue resolution combined with its perfusion parameters to determine the probability of positive PLC. The employed Siemens GRASP DCE application scanner is equipped with a BioMatrix system for compressed sensing imaging, and a radial acquisition method with a 111.25° golden angle K-space filling method was applied, allowing patients to provide high signal-to-noise ratio images without breath holding, achieving high temporal and

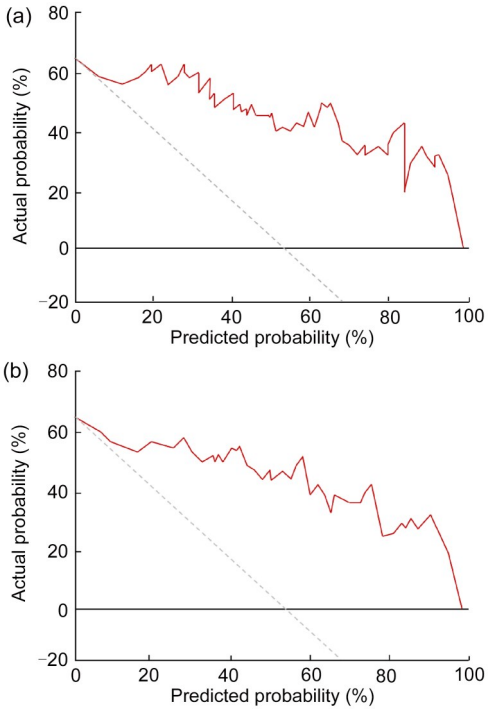

Fig. 6 Decision curve analyses of peritoneal lavage cytology (PLC)-positive nomogram of gastric cancer patients. (a) Modeling group; (b) Validation group.

spatial resolution scans (Benkert et al., 2018), and greatly improving the accuracy of quantitative blood flow dynamics in gastric cancer (Li et al., 2018). Logistic regression analysis showed that the T stage, tumor thickness, and perfusion parameter K_{trans} of gastric cancer GRASP DCE-MRI were independent predictors of PLC positivity, which were used to construct a column chart predicting the PLC positivity rate. The efficacy of the model was confirmed in the validation group.

The transfer constant K_{trans} among the MR perfusion parameters refers to the rate constant of contrast agent molecules moving from the intravascular space to the extravascular interstitial space, which is related to the permeability of blood vessels and the surface area of endothelial cells. The data from this study showed that the K_{trans} value in the experimental group of gastric cancer patients who had a positive result in the peritoneal lavage fluid was significantly higher than that in the negative group, and K_{trans} was related to the histological differentiation degree, consistent with previous domestic and foreign studies (la Torre et al., 2010; Song and Xue, 2015), suggesting that the higher the malignancy degree of advanced gastric cancer tumor, the faster the rate of intravascular substance permeation into the tissue interstitium. Possibly due to the incomplete structure of neovascular walls in gastric cancer tissue, the higher the malignancy degree, the stronger the vascular permeability, and the greater the risk of cancer cells traveling through the bloodstream. V_e indirectly reflects the permeability of the vascular wall in the extravascular interstitial space, and K_{ep} refers to the rate at which the contrast agent returns to the intravascular space. There was no statistically significant difference in V_e or K_{ep} between the positive and negative groups in the modeling group, possibly due to the complex texture of the tumors and the uneven distribution of necrosis, resulting in an inconsistent extracellular environment of tumor cells. Further research is needed to clarify this result.

In this study, the accuracy of MR TN staging for gastric cancer was greatly improved in terms of postoperative pathological gold standard compared to other imaging examinations. Preoperative tumor staging was based on CT, and it showed that the specificity of predicted results was less than 60% (Xu et al., 2019). The conventional staging sensitivity of MR is also unsatisfactory (Huang et al., 2015). Although positron emission tomography (PET)-CT improves sensitivity to about 70% (Brenkman et al., 2018), its specificity is still lower than that of our findings (78.5%). This illustrates the tremendous value of GRASP DCE technology in tumor staging of preoperative application for gastric cancer.

Clinical practice and previous studies have confirmed the correlation between T stage and peritoneal implantation metastasis (de Andrade and Mezhir, 2014). The MRI TN stage was included as a variable in our study, and the differences between positive and negative PLC results were analyzed. The statistical results showed that the MRI T stage level was a significant predictor of positive peritoneal lavage fluid, consistent with previous findings (Song and Xue, 2015), while the N stage of MRI and postoperative pathology had no correlation with the results of peritoneal lavage fluid, indicating that lymph node metastasis may not directly affect tumor hematogenous metastasis or the shedding of malignant cells on the serosal surface, which is inconsistent with the previous results reported by Yue et al. (2017). We will continue to evaluate and verify this issue by expanding the sample size.

The present study considered tumor thickness instead of tumor size, as gastric cancer tumors are irregular in shape and infiltrated in the stomach wall with

multiple creeping, making the surface area of the tumor difficult to measure. Meanwhile, tumor thickness can reflect the tumor's growth status and malignant degree to some extent (Tsuda et al., 1995). In future studies, we will attempt to use third-party software to assist in measuring tumor volume or surface area to further improve research accuracy.

Studies have demonstrated that diffuse-type gastric cancer in the Lauren classification is more prone to infiltration and peritoneal metastasis than other types (Ma et al., 2017; del Arco et al., 2022), consistent with our results. The possible reason is that diffuse-type gastric cancer tissue lacks a clear epithelial belt, with cancer cells individually wrapped in fibrous connective tissue, resulting in poor adhesion and a higher risk of shedding. In this study, the K_{trans} value in diffuse-type gastric cancer was higher than those in other types, possibly due to more inflammation and edema or connective tissue proliferation in other types (Ma et al., 2016), affecting vascular permeability and therefore the contrast agent's penetration rate. If preoperative endoscopic pathology can obtain the gastric cancer Lauren classification and include it in regression analysis, the prediction results may become more accurate.

Japanese guidelines have indicated that the treatments of gastrectomies performed by PLC-positive patients were non-radical operations (Japanese Gastric Cancer Association, 2021), suggesting the addition of neoadjuvant chemotherapy. Based on these guidelines and the findings of this study, we conclude that additional neoadjuvant chemotherapy could be considered to improve treatment outcomes for patients with gastric cancer who are staged as T_4 and have a thickness greater than 20 mm and a K_{trans} value greater than or equal to 0.4 min^{-1}, as determined by GRASP DCE-MRI.

There are several limitations of this study. Firstly, this was a single-center study, and hence the results may be biased to a certain extent. Additionally, the adopted PLC test has a certain false-negative rate. Literature has shown that PCR and other detection techniques can improve the positive detection rate of shed cells (Ito et al., 2005; Xiao et al., 2014). In future experiments, we will use more accurate PLC detection technology to further improve the reliability of the predictions. Although the MRI parameters generated by this study had a favorable predictive performance, further case verification is still needed to validate its predictive ability. We will continue to recruit patients and expand the sample size, and also try to use third-party software to quantify the MRI signal and establish an automatic staging model, in order to conduct a more accurate prediction of peritoneal metastasis of gastric cancer in combination with perfusion. Further case verification is still needed to validate the predictive ability of GRASP DCE-MRI.

In summary, GRASP DCE-MRI and perfusion parameters could predict the probability of peritoneal free cancer cells in patients with gastric cancer. The nomogram model constructed using these predictors may help clinicians to better predict the risk of peritoneal free cancer cells in gastric cancer patients and guide clinical decision-making. Therefore, this non-invasive method has the potential to improve patient outcomes.

Data availability statement

The data that support the findings of this study are not openly available due to reasons of sensitivity and are available from the corresponding author upon reasonable request. Data are located in controlled access data storage at the First Affiliated Hospital of Ningbo University (Ningbo, China).

Acknowledgments

This work was supported by the Ningbo Public Welfare Fund (No. 2021S185). We thank Dr. Zhebin DONG (Department of Gastrointestinal Surgery, Ningbo Medical Center Lihuili Hospital, Ningbo, China) for providing a great deal of help in drawing charts.

Author contributions

Xueqing YIN performed the experimental research and data analysis, wrote and edited the manuscript. Xinzhong RUAN performed the investigation of PLC models. Yongmeng ZHU provided resources and images acquisition. Yongfang YIN contributed to case acquisition and performed supplementary operations for peritoneal lavage. Rui HUANG performed data measurement and data curation. Chao LIANG supported on methodology and review of the manuscript. All authors have read and approved the final manuscript, and therefore, have full access to all the data in the study and take responsibility for the integrity and security of the data.

Compliance with ethics guidelines

Xueqing YIN, Xinzhong RUAN, Yongmeng ZHU, Yongfang YIN, Rui HUANG, and Chao LIANG declare that they have no conflict of interest.

All procedures followed were in accordance with the ethical standards of the responsible committee on human experimentation (institutional and national) and with the Helsinki

Declaration of 1975, as revised in 2013. Informed consent was obtained from all patients for being included in the study. Additional informed consent was obtained from all patients for whom identifying information is included in this article.

References

Bell LK, Ainsworth NL, Lee SH, et al., 2011. MRI & MRS assessment of the role of the tumour microenvironment in response to therapy. *NMR Biomed*, 24(6):612-635. https://doi.org/10.1002/nbm.1720

Benkert T, Tian Y, Huang CC, et al., 2018. Optimization and validation of accelerated golden-angle radial sparse MRI reconstruction with self-calibrating GRAPPA operator gridding. *Magn Reson Med*, 80(1):286-293. https://doi.org/10.1002/mrm.27030

Borggreve AS, Goense L, Brenkman HJF, et al., 2019. Imaging strategies in the management of gastric cancer: current role and future potential of MRI. *Br J Radiol*, 92(1097): 20181044. https://doi.org/10.1259/bjr.20181044

Brenkman HJF, Gertsen EC, Vegt E, et al., 2018. Evaluation of PET and laparoscopy in staging advanced gastric cancer: a multicenter prospective study (PLASTIC-study). *BMC Cancer*, 18:450. https://doi.org/10.1186/s12885-018-4367-9

Chandarana H, Feng L, Block TK, et al., 2013. Free-breathing contrast-enhanced multiphase MRI of the liver using a combination of compressed sensing, parallel imaging, and golden-angle radial sampling. *Invest Radiol*, 48(1):10-16. https://doi.org/10.1097/RLI.0b013e318271869c

de Andrade JP, Mezhir JJ, 2014. The critical role of peritoneal cytology in the staging of gastric cancer: an evidence-based review. *J Surg Oncol*, 110(3):291-297. https://doi.org/10.1002/jso.23632

del Arco CD, Muñoz LE, Medina LO, et al., 2022. Clinicopathological differences, risk factors and prognostic scores for western patients with intestinal and diffuse-type gastric cancer. *World J Gastrointest Oncol*, 14(6):1162-1174. https://doi.org/10.4251/wjgo.v14.i6.1162

Feng L, 2022. Golden-angle radial MRI: basics, advances, and applications. *J Magn Reson Imaging*, 56(1):45-62. https://doi.org/10.1002/jmri.28187

Feng L, Grimm R, Block KT, et al., 2014. Golden-angle radial sparse parallel MRI: combination of compressed sensing, parallel imaging, and golden-angle radial sampling for fast and flexible dynamic volumetric MRI. *Magn Reson Med*, 72(3):707-717. https://doi.org/10.1002/mrm.24980

Huang Z, Xie DH, Guo L, et al., 2015. The utility of MRI for pre-operative T and N staging of gastric carcinoma: a systematic review and meta-analysis. *Br J Radiol*, 88(1050): 20140552. https://doi.org/10.1259/bjr.20140552

Ito S, Nakanishi H, Kodera Y, et al., 2005. Prospective validation of quantitative CEA mRNA detection in peritoneal washes in gastric carcinoma patients. *Br J Cancer*, 93(9): 986-992. https://doi.org/10.1038/sj.bjc.6602802

Jamel S, Markar SR, Malietzis G, et al., 2018. Prognostic significance of peritoneal lavage cytology in staging gastric cancer: systematic review and meta-analysis. *Gastric Cancer*, 21(1):10-18. https://doi.org/10.1007/s10120-017-0749-y

Japanese Gastric Cancer Association, 2011. Japanese classification of gastric carcinoma: 3rd English edition. *Gastric Cancer*, 14(2):101-112. https://doi.org/10.1007/s10120-011-0041-5

Japanese Gastric Cancer Association, 2021. Japanese gastric cancer treatment guidelines 2018 (5th edition). *Gastric Cancer*, 24(1):1-21. https://doi.org/10.1007/s10120-020-01042-y

la Torre M, Ferri M, Giovagnoli MR, et al., 2010. Peritoneal wash cytology in gastric carcinoma. Prognostic significance and therapeutic consequences. *Eur J Surg Oncol*, 36(10):982-986. https://doi.org/10.1016/j.ejso.2010.06.007

Leach MO, Morgan B, Tofts PS, et al., 2012. Imaging vascular function for early stage clinical trials using dynamic contrast-enhanced magnetic resonance imaging. *Eur Radiol*, 22(7):1451-1464. https://doi.org/10.1007/s00330-012-2446-x

Li HH, Zhu H, Yue L, et al., 2018. Feasibility of free-breathing dynamic contrast-enhanced MRI of gastric cancer using a golden-angle radial stack-of-stars VIBE sequence: comparison with the conventional contrast-enhanced breath-hold 3D VIBE sequence. *Eur Radiol*, 28(5):1891-1899. https://doi.org/10.1007/s00330-017-5193-1

Ma JL, Shen H, Kapesa L, et al., 2016. Lauren classification and individualized chemotherapy in gastric cancer. *Oncol Lett*, 11(5):2959-2964. https://doi.org/10.3892/ol.2016.4337

Ma L, Xu XW, Zhang M, et al., 2017. Dynamic contrast-enhanced MRI of gastric cancer: correlations of the pharmacokinetic parameters with histological type, Lauren classification, and angiogenesis. *Magn Reson Imaging*, 37:27-32. https://doi.org/10.1016/j.mri.2016.11.004

Mezhir JJ, Shah MA, Jacks LM, et al., 2010. Positive peritoneal cytology in patients with gastric cancer: natural history and outcome of 291 patients. *Ann Surg Oncol*, 17(12): 3173-3180. https://doi.org/10.1245/s10434-010-1183-0

Offersen BV, Borre M, Overgaard J, 2003. Quantification of angiogenesis as a prognostic marker in human carcinomas: a critical evaluation of histopathological methods for estimation of vascular density. *Eur J Cancer*, 39(7):881-890. https://doi.org/10.1016/s0959-8049(02)00663-9

Oh-E H, Tanaka S, Kitadai Y, et al., 2001. Angiogenesis at the site of deepest penetration predicts lymph node metastasis of submucosal colorectal cancer. *Dis Colon Rectum*, 44(8):1129-1136. https://doi.org/10.1007/BF02234633

Riihimäki M, Hemminki A, Sundquist K, et al., 2016. Metastatic spread in patients with gastric cancer. *Oncotarget*, 7(32):52307-52316. https://doi.org/10.18632/oncotarget.10740

Song SB, Xue YW, 2015. Clinicopathological factor analysis of positive cells in peritoneal lavage of gastric carcinoma. *Chin J Gastrointest Surg*, 18(11):1128-1131 (in Chinese). https://doi.org/10.3760/cma.j.issn.1671-0274.2015.11.015

Sun F, Feng M, Guan WX, 2017. Mechanisms of peritoneal dissemination in gastric cancer (review). *Oncol Lett*, 14(6): 6991-6998. https://doi.org/10.3892/ol.2017.7149

Teo QQ, Thng CH, Koh TS, et al., 2014. Dynamic contrast-enhanced magnetic resonance imaging: applications in oncology. *Clin Oncol (R Coll Radiol)*, 26(10):e9-e20. https://doi.org/10.1016/j.clon.2014.05.014

To EMC, Chan WY, Chow C, et al., 2003. Gastric cancer cell detection in peritoneal washing: cytology versus RT-PCR for CEA transcripts. *Diagn Mol Pathol*, 12(2):88-95. https://doi.org/10.1097/00019606-200306000-00004

Tsuda K, Hori S, Murakami T, et al., 1995. Intramural invasion of gastric cancer: evaluation by CT with water-filling method. *J Comput Assist Tomogr*, 19(6):941-947. https://doi.org/10.1097/00004728-199511000-00019

Valletti M, Eshmuminov D, Gnecco N, et al., 2021. Gastric cancer with positive peritoneal cytology: survival benefit after induction chemotherapy and conversion to negative peritoneal cytology. *World J Surg Oncol*, 19:245. https://doi.org/10.1186/s12957-021-02351-x

Wang YD, Wu P, Mao JD, et al., 2007. Relationship between vascular invasion and microvessel density and micrometastasis. *World J Gastroenterol*, 13(46):6269-6273. https://doi.org/10.3748/wjg.v13.i46.6269

Weidner N, 1998. Tumoural vascularity as a prognostic factor in cancer patients: the evidence continues to grow. *J Pathol*, 184(2):119-122. https://doi. org/10.1002/(SICI)1096-9896(199802)184:2<119::AID-PATH17>3.0.CO;2-D

Wu CC, Li MN, Meng HB, et al., 2019. Analysis of status and countermeasures of cancer incidence and mortality in China. *Sci China Life Sci*, 62(5):640-647. https://doi.org/10.1007/s11427-018-9461-5

Xiao Y, Zhang J, He X, et al., 2014. Diagnostic values of carcinoembryonic antigen in predicting peritoneal recurrence after curative resection of gastric cancer: a meta-analysis. *Ir J Med Sci*, 183(4):557-564. https://doi.org/10.1007/s11845-013-1051-6

Xu SH, Feng LL, Chen YM, et al., 2019. Study on the sensitivity of multi-slice spiral CT in diagnosis of lymph node metastasis in different lymph node stations of gastric cancer. *Chin J Gastrointest Surg*, 22(10):984-989 (in Chinese). https://doi.org/10.3760/cma.j.issn.1671-0274.2019.10.015

Yashiro M, Chung YS, Nishimura S, et al., 1996. Fibrosis in the peritoneum induced by Scirrhous gastric cancer cells may act as "soil" for peritoneal dissemination. *Cancer*, 77(8):1668-1675. https://doi.org/10.1002/(SICI)1097-0142(19960415)77:8<1668::AID-CNCR37>3.0.CO;2-W

Yue J, Duan XF, Gong L, et al., 2017. Lymph node metastasis regularity and risk factors in 768 cardiac carcinoma patients. *Chin J Gastrointest Surg*, 20(11):1283-1287 (in Chinese). https://doi.org/10.3760/cma.j.issn.1671-0274.2017.11.015